ELSEVIER

Chemical Physics 219 (1997) 161–172

Chemical Physics

Inclusion of ion-pair states in the diatomics-in-molecules description of potential energy surfaces: van der Waals complexes of $He-Cl_2$ and $Ar-Cl_2$

B.L. Grigorenko [a], A.V. Nemukhin [a], V.A. Apkarian [b,*]

[a] *Department of Chemistry, Moscow State University, Moscow 119899, Russian Federation*
[b] *Department of Chemistry, University of California, Irvine, CA 926192-2025, USA*

Received 14 January 1997

Abstract

It is shown that the inclusion of excited ionic configurations in the diatomics-in-molecules (DIM) Hamiltonian serves as a natural means to account for main features of non-additivity in three-body potential energy surfaces of $He-Cl_2$ and $Ar-Cl_2$ van der Waals complexes. For ground state $Cl_2(^1\Sigma_g)$, while consideration of only neutral configurations leads to T-shaped isomers, inclusion of the excited Cl^+Cl^- configuration stabilizes the linear isomer and destabilizes the T-shaped isomer. Within the same formalism, the excited $Cl_2(^3\Pi)$ only sustains minima in the T-shaped isomer. Potential energy surfaces created with a minimal DIM basis are constructed and shown to compare favorably with the most accurate ab initio surfaces and experiments. Analytical forms are given for the three-body surfaces, meant for fitting purposes and as a convenience in simulations of dynamics. © 1997 Elsevier Science B.V.

1. Introduction

The aim of this work is to study the effect of including ionic configurations on the diatomics-in-molecules (DIM) construct of potential energy surfaces for van der Waals complexes. We will take as our specific examples the $HeCl_2$ and $ArCl_2$ complexes, in which the ionic configurations of importance are the molecular, Cl^+Cl^-, ion-pair states. Three principal starting points motivate this study.

From the viewpoint of identifying many-body contributions to interaction potentials, as they arise in condensed phase systems, we are interested in establishing a hierarchy of approximations based on sound physical principles and transparent insights. Different approaches, therefore different languages, can be used for such formulations. The energy decomposition analysis of Morokuma [1], the natural bond orbital analysis of Weinhold and coworkers [2], and perturbation theory-based formalisms [3–8], are examples. We have chosen the DIM framework for our approach, and consider the extent to which 'non-additive' contributions to many-body interactions can be reproduced with information solely derived from a knowledge of the constituent

* Corresponding author.

PII S0301-0104(97)00107-9

pair potentials. Given the fact that information about diatomic fragments can be derived with high levels of accuracy, properly devised schemes for using such information in treating extended systems is of general and practical value. An analysis of the $HeCl_2$ potential energy surface both in the ground (X) and excited (B) electronic states of the molecule was recently reported [9]. There, the DIM method was applied with a complete set of polyatomic basis functions arising from the lowest energy states of the atoms $Cl(^2P)$ and $He(^1S)$. Several levels of the theory, based on inclusion of various contributions to the interaction potential were tested. It was discovered that the greatest impact on the shape of the potential energy surface, in particular in the regions of the potential wells, stems from the very first step in the procedure, when the pairwise potential is extended to include the anisotropy of the He–Cl interaction. Other refinements within this limited basis lead to less noticeable changes. In the present work, we consider the effect of augmenting the DIM basis set to include ion-pair states while at the same time reducing the matrix of neutral states to a bare minimum. We show, that the inclusion of a single ion-pair configuration, together with the anisotropy of covalent interactions, leads to a significant improvement of the three-body surfaces.

The importance of ion-pair states in the DIM description of polyatomics has been highlighted before. In previous DIM applications it has been shown that the inclusion of ionic states is essential for the correct prediction of equilibrium geometries in molecules of partly ionic bonding character [10,11]. The same has been clearly emphasized in the diatomics-in-ionic-systems (DIIS) treatment of halogens in rare gas solids by Last and George, and coworkers [12–14]. Our recent calculations on van der Waals clusters of $HFAr_n$ [15], and $(HF)_2Ar_n$ [16], demonstrated the utility of DIM-based Ar–HF three-body surfaces which were constructed by inclusion of ionic states. The crucial contribution of the latter to produce an acceptable three-body ground surface was detailed through comparisons with the accurate ab initio and empirical potentials for the same system. While the strategy of including ion-pair states in the DIM matrix has been demonstrated to be useful in constructing three-body surfaces, it must be appreciated that they will have a more profound effect in condensed phase treatments. Due to the long-range nature of ionic potentials, they are subject to truly many-body solvation in a fundamentally different way than neutrals which are dominated by short range interactions. The admixture of ionic configurations in ground state electronic surfaces can therefore be expected to have dramatic effects in the non-additivity of potentials constructed from neutral fragments alone.

Finally, the structure of vdW complexes between rare gas atoms and molecular halogens, $Rg–X_2$ (where X is a halogen atom), has been the subject of extensive deliberation. In the electronic ground state, two competing geometries of these complexes are at issue: T-shaped vs. linear. Given the very weak binding in these complexes, it is not too surprising that the precise distinction between the two possible isomers is a serious challenge to theory. According to most recent high level ab initio calculations the potential minimum for the linear Rg–X–X configuration is ≈ 5–7% lower than that of the T-shaped structure [3,4,7,8]. Despite this, due to the consideration of zero-point energies, the ground state wavefunction in $He–Cl_2$ is localized in the T-well, consistent with experiment [3,4]. At the same level of theory, the same type of compensation does not occur in the case of the heavier $Ar–Cl_2$ complex, where the predicted minimum energy structure is linear, in apparent contradiction with experiment [3,4]. At much higher levels of theory, the linear well while deeper, approaches the T-minimum, to now favor the T-structure when the zero-point effect comes into play [4]. Quite clearly, the use of isotropic atom–atom potentials can only yield the T-shaped isomer for the van der Waals complex. The additional linear minima can only arise when anisotropic Rg–X pair potentials are considered, as illustrated by Naumkin and Knowles for $Ar–X_2$ surfaces [17]. These treatments can be regarded as the lowest in the hierarchy of DIM constructs, as already elaborated [9]. However, even with the use of the more complete treatment, including all 36 molecular halogen states in the DIM basis, in the case of $He–Cl_2$, the minimum for the linear geometry is essentially absent [9]. As surmised, the incorporation of ionic configurations in the DIM basis changes this situation.

In this work, we first consider the effect of ionic contributions on the singlet ground state surface of $Rg–Cl_2$ by taking the minimal basis set required for such a treatment. We include in the DIM set of polyatomic basis functions the lowest energy ion-pair states which mix with the ground state, namely, states derived from the

$Cl^-(^1S) + Cl^+(^1D)$ ionic terms, along with the lowest neutral states arising from $Cl(^2P)$ and $Rg(^1S)$. We use the construct to compute the $ArCl_2$ and $HeCl_2$ surfaces and compare them to the accurate potentials which have been critically analyzed recently [3,4]. We then consider the van der Waals complex between an excited state $Cl_2(^3\Pi)$ and Ar, in which the contributing ionic configuration is the $Cl^+Cl^-(^3\Pi)$ arising from the $Cl^+(^3P) + Cl^-(^1S)$ limit. In contrast with the ground state, the excited state surface sustains only a T-shaped minimum, and DIM analysis provides the insights for this distinction. We should perhaps emphasize at the onset, that we do not expect to match the accuracy of the existing ab initio calculations. Our aim is to provide a simple physical picture for the subtleties of the surfaces, and to provide a qualitatively accurate functional forms that are useful in treatments of many-body dynamics.

2. Theory

According to the DIM strategy the Hamiltonian for the three atomic system $Rg–X_2$ is written as follows:

$$H = \sum_a \sum_{b>a} H^{(ab)} - (N-2)\sum_a H^{(a)}. \tag{1}$$

This Hamiltonian should be converted into the matrix form for the specified set of polyatomic basis functions (PBF) Φ_i. In this application, i.e. for the $1A'$ symmetry of $RgCl_2$, the PBF set is constructed from the lowest energy atomic functions of neutral, $Cl(^2P)$, $Rg(^1S)$, as well as of ionic states, $Cl^+(^1D)$, $Cl^-(^1S)$ for the singlet matrix, and $Cl^+(^3P)$, $Cl^-(^1S)$ in the case of the triplet matrix. The PBF set and corresponding symmetries of diatomic states contributing to the fragment Hamiltonian operators are collected in Table 1.

We apply here the simplest version of the DIM formalism [18], one that does not allow us to distinguish all states of Cl_2 within the $D_{\infty h}$ group (e.g. g or u symmetries are not specified). Although refinement of the formalism is straightforward [9,19], it would defeat our minimalist purpose. The coordinate system used in our notation is illustrated in Fig. 1. One chlorine atom, $Cl^{(1)}$, is located at the origin, and the second atom $Cl^{(2)}$ lies on the z-axis. The angles ϕ_i $(i = 1, 2)$ designate the angles between the z-axis and $Cl^{(i)}$-Rg directions.

Table 1
Composition of polyatomic basis functions, Φ_i, in terms of atomic states and corresponding diagonal matrix elements of diatomic fragments

i	Rg	$Cl^{(1)}/Cl^+/Cl^-$	$Cl^{(2)}/Cl^-/Cl^+$	$V_{ii}(Cl^{(1)}Cl^{(2)})$	$V_{ii}(Cl^{(1)}Rg)$	$V_{ii}(Cl^{(2)}Rg)$
(a) $Cl_2(X^1\Sigma_g)$–Rg						
1	^1S	^2P_x	^2P_x	$^1\Delta(Cl_2)$	$^2\Pi$(Cl Rg)	$^2\Pi$(Cl Rg)
2	^1S	^2P_z	^2P_x	$^1\Pi(Cl_2)$	$^2\Sigma$(Cl Rg)	$^2\Pi$(Cl Rg)
3	^1S	^2P_x	^2P_z	$^1\Pi(Cl_2)$	$^2\Pi$(Cl Rg)	$^2\Sigma$(Cl Rg)
4	^1S	^2P_z	^2P_z	$^1\Sigma(Cl_2)$	$^2\Sigma$(Cl Rg)	$^2\Sigma$(Cl Rg)
5	^1S	$^1D_{zz}$	^1S	$^1\Sigma(Cl^+Cl^-)$	$^1\Sigma(Cl^+$ Rg)	$^1\Sigma(Cl^-$ Rg)
6	^1S	$^1D_{xz}$	^1S	$^1\Pi(Cl^+Cl^-)$	$^1\Pi(Cl^+$ Rg)	$^1\Sigma(Cl^-$ Rg)
7	^1S	$^1D_{xx-yy}$	^1S	$^1\Delta(Cl^+Cl^-)$	$^1\Delta(Cl^+$ Rg)	$^1\Sigma(Cl^-$ Rg)
8	^1S	^1S	$^1D_{zz}$	$^1\Sigma(Cl^-Cl^+)$	$^1\Sigma(Cl^-$ Rg)	$^1\Sigma(Cl^+$ Rg)
9	^1S	^1S	$^1D_{xz}$	$^1\Pi(Cl^-Cl^+)$	$^1\Sigma(Cl^-$ Rg)	$^1\Pi(Cl^+$ Rg)
10	^1S	^1S	$^1D_{xx-yy}$	$^1\Delta(Cl^-Cl^+)$	$^1\Sigma(Cl^-$ Rg)	$^1\Delta(Cl^+$ Rg)
(b) $Cl_2(^3\Pi_u)$–Rg						
1	^1S	^2P_x	^2P_x	$^3\Delta(Cl_2)$	$^2\Pi$(Cl Rg)	$^2\Pi$(Cl Rg)
2	^1S	^2P_z	^2P_x	$^3\Pi(Cl_2)$	$^2\Sigma$(Cl Rg)	$^2\Pi$(Cl Rg)
3	^1S	^2P_x	^2P_z	$^3\Pi(Cl_2)$	$^2\Pi$(Cl Rg)	$^2\Sigma$(Cl Rg)
4	^1S	^2P_z	^2P_z	$^3\Sigma(Cl_2)$	$^2\Sigma$(Cl Rg)	$^2\Sigma$(Cl Rg)
5	^1S	$^1S(Cl^-)$	$^3P_y(Cl^+)$	$^3\Pi Cl^+Cl^-)$	$^1\Sigma(Cl^-$ Rg)	$^3\Pi(Cl^-$ Rg)
6	^1S	$^3P_y(Cl^+)$	$^1S(Cl^-)$	$^3\Pi(Cl^+Cl^-)$	$^3\Pi(Cl^+$ Rg)	$^1\Sigma(Cl^-$ Rg)

The fragment Hamiltonian matrices are given as:

$$\begin{aligned} \mathbf{H}^{(Cl_2)} &= \mathbf{B}_{Cl_2}^{-1}\mathbf{V}(Cl_2)\mathbf{B}_{Cl_2} \\ \mathbf{H}^{(Cl^{(i)}Rg)} &= \left[\mathbf{R}_{Cl^{(i)}}^{Cl_2}\right]^{*}\mathbf{V}(Cl^{(i)}Rg)\mathbf{R}_{Cl^{(i)}}^{Cl_2} \\ \mathbf{H}^{(Rg)} &= \mathbf{V}(Rg) \\ \mathbf{H}^{(Cl^{(i)})} &= \mathbf{V}(Cl^{(i)}) \end{aligned}, \tag{2}$$

where all $\mathbf{V}$ matrices are diagonal, containing energies of the diatomic and atomic states (Table 1). The rotation matrices $\mathbf{R}$, rotate the quantization axis from the Rg–Cl direction to the reference frame of the molecular halogen, specifically, for $i = 1$:

$$\mathbf{R}_{Cl^{(i)}}^{Cl_2} = \begin{bmatrix} \cos\phi_1 & \sin\phi_1 & & & & & & & \\ -\sin\phi_1 & \cos\phi_1 & & & & & & & \\ & & \cos\phi_1 & \sin\phi_1 & & & & & \\ & & -\sin\phi_1 & \cos\phi_1 & & & & & \\ & & & & \frac{1}{2}(3\cos^2\phi_1 - 1) & -\sqrt{3}\cos\phi_1\sin\phi_1 & -\frac{1}{2}\sqrt{3}\sin^2\phi_1 & & \\ & & & & \sqrt{3}\cos\phi_1\sin\phi_1 & \cos^2\phi_1 - \sin^2\phi_1 & -\sin\phi_1\cos\phi_1 & & \\ & & & & \frac{1}{2}\sqrt{3}\sin^2\phi_1 & \sin\phi_1\cos\phi_1 & \frac{1}{2}(1+\cos^2\phi_1) & & \\ & & & & & & & 1 & \\ & & & & & & & & 1 \\ & & & & & & & & & 1 \end{bmatrix}. \tag{3}$$

The matrix $\mathbf{B}$ is responsible for mixing the diatomic states of the same spin and spatial symmetry, here, the mixing is between the three $^1\Sigma$ states of Cl_2 (see Table 1 (a)). Most generally, the 3×3 non-unit block of the orthogonal matrix $\mathbf{B}$ contains three mixing parameters α, β, γ:

$$\mathbf{B} = \begin{bmatrix} \cos\alpha\cos\gamma - \cos\beta\sin\alpha\sin\gamma & \cos\alpha\sin\gamma + \cos\beta\cos\gamma\sin\alpha & \sin\alpha\sin\beta \\ -\sin\alpha\cos\gamma - \cos\beta\cos\alpha\sin\gamma & -\sin\alpha\sin\gamma + \cos\beta\cos\gamma\cos\alpha & \cos\alpha\sin\beta \\ \sin\beta\sin\gamma & -\sin\beta\cos\gamma & \cos\beta \end{bmatrix}. \tag{4}$$

We simplify the problem by setting $\alpha = \gamma = \pi/4$, and by estimating β from electronic structure calculations. To this end, we created a set of molecular orbitals for the Cl_2 molecule at its equilibrium position, then

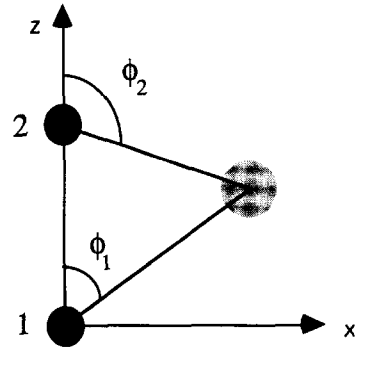

Fig. 1. Coordinate system used for the Rg–Cl_2 complex.

transform these orbitals to a set of natural atomic orbitals, namely, the localized atom centered one electron functions [2]. With this set of orbitals we performed the CI calculation when distributing all valence electrons over all valence orbitals of the molecule. Analyzing the multiconfigurational wavefunctions we concluded that the weight of the covalent contribution in the ground state of Cl_2 is approximately 0.8, and the ionic contribution is about 0.2, i.e. $\beta = 25°$.

Finally, as already discussed in our previous work on the Ar–HF DIM potential energy surface, the potential matrix elements for the ion-pair states should be summed vectorially, as the sum of ion–atom interactions [15]. Restricting this interaction to the leading electrostatic term of charge-induced dipole, it is convenient to use scalar pair potentials for the ion–atom interactions and to correct for the combined action of two oppositely charged centers, here Cl^- and Cl^+, with the correction term given as:

$$\Delta V_{\text{ion}} = \alpha(\text{Rg}) \frac{\left(\bar{R}_{\text{RgCl}^{(1)}} \bar{R}_{\text{RgCl}^{(2)}}\right)}{R^3_{\text{RgCl}^{(1)}} R^3_{\text{RgCl}^{(2)}}} . \tag{5}$$

3. Diatomic input

For the Rg–Cl interactions we use the experimentally determined adiabatic potential curves for the Σ and Π states which were derived by Aquilanti et al. from measurements of total scattering cross-sections [20]. We use their fits for the $^2\Sigma$ and $^2\Pi$ states of He–Cl, Ar–Cl in the form of the MSV (Morse–Spline–van der Waals) parametrization for isotropic part of the interaction and the Buckingham form for the anisotropic component [20].

For $He–Cl^-(^1S)$, and $Ar–Cl^-(^1S)$ potentials we use the extended Tang–Toennies (ETT) potentials which are based on a combination of SCF calculations at short range, and scaled induction and dispersion terms up to R^{-10} for long range interactions [21].

For the $Rg–Cl^+$ system, we are only aware of the paper by Balasubramanian et al. on $Ar–Cl^+$ [22]. They use the relativistic pseudopotential developed by Pacios and Christiansen [23], and use the corresponding [3s3p1d] basis sets within the first order configuration interaction (FOCI) scheme followed by the valence shell CASSCF procedure. We recalculated the $^1\Sigma$, $^1\Pi$, $^1\Delta$ states of $Ar–Cl^+(^1D)$, along with those of $He–Cl^+(^1D)$ by using an advanced procedure. Namely, the diatomic energies are computed with the help of second order CI (SOCI), taking into account single and double excitations from the set of reference configurations which in turn account for complete distribution of valence electrons over valence orbitals. The calculations were carried out with the

Table 2
Coefficients of the fitting function, Eq. (6) in text, for the Cl^+–Rg potentials. Distances are in a.u., energies are in atomic units

		A (au)	a (1/au)	B (1/au)	C (1/au^2)	D (1/au^3)	Limits
$HeCl^+$	$^1\Sigma$	3.924×10^{-2}	1.356	8.5	−2.21	−0.08	$r > 2.5$ Å
	$^1\Pi$	0.2528	1.680	16.59	−2.07	−0.22	$r > 2.5$ Å
	$^1\Delta$	0.4873	1.712	19.29	−1.90	−0.21	$r > 2.5$ Å
$ArCl^+$	$^1\Sigma$	9.976×10^{-3}	0.863	−44.72	−8.21	1.78	$r > 2.5$ Å
	$^1\Pi$	3.641	1.178	4.080	−1.58	0.14	$r > 2.6$ Å
	$^1\Delta$	0.2874	1.768	168.4	−5.36	0.04	$r > 2.5$ Å
	$^3\Pi$	2.022	1.240	5.20	−2.02	0.18	$r > 2.7$ Å

Table 3
Parameters (well depth and equilibrium positions) of diatomic potentials used in the calculations. R_m values are given in Å, the ε values are in cm^{-1}

		Cl–Rg [20]		Cl^+–Rg				Cl^-–Rg [21]
		Σ	Π	$^1\Sigma$	$^1\Pi$	$^1\Delta$	$^3\Pi$	Σ
He	R_m	3.39	3.53	1.6	2.8	3.5		4.1
	ε	25	20	1400	209	92		44
Ar	R_m	3.68	3.96	2.16	2.6	4.0	2.71	3.74
	ε	141	92	11670	4333	135	2581	518

GAMESS program system [24]. In the case of Ar–Cl^+ the same pseudopotentials and basis sets as in Ref. [22] were used. For He–Cl^+ the all electron treatment was employed with the following basis sets: [6s3p1d] for He borrowed from Refs. [25–27] and [6s6p2d] for Cl from Ref. [28]. The computed points were then fitted in the relevant range of importance to the form:

$$V = Ae^{-ar}(1 + Br + Cr^2 + Dr^3) - \frac{0.5\alpha}{r^4}, \tag{6}$$

in which α is the polarizability of the rare gas atom (1.38 au for He, and 11.1 au for Ar). Table 2 gives the fitting parameters A, a, B, C, D of Eq. (6), along with the corresponding interpolation boundaries. For convenience, we have collected in Table 3 the well depths and equilibrium positions of all potentials used in these calculations. Note, the $ArCl^+(^3\Pi)$ parameters are directly taken from Ref. [22].

For the excited states of Cl_2, namely, $^1\Pi$ and $^1\Delta$ states correlating with the ground states of neutral Cl atoms, as well as for $^1\Sigma$, $^1\Pi$, $^1\Delta$ states correlating with the Cl^-–Cl^+ limit we use the potentials given by Peyerimhoff and Buenker [28].

Table 4
Stationary points computed with the various DIM approximations: the equilibrium distances, R_e, are from the center of mass of Cl_2 to Rg in the equilibrium geometry, and the binding energies, D_e, are referenced to the Cl_2–Rg at infinite separation. The two last lines of the table show the literature values obtained with ab initio potentials. R_e values are given in Å, and D_e in cm^{-1}

		He–Cl_2		Ar–Cl_2	
		L	T	L	T
Scheme A	R_e	–	3.25	–	3.55
	D_e		50.2		283.
Scheme B	R_e	4.4	3.4	4.65	3.8
	D_e	27.6 [a]	40.5	154.	188.
Scheme C	R_e	4.55	3.58	4.5	3.88
	D_e	25.1	31.4	212.	134
Refs. [6–8]	R_e	4.25	3.5	4.5	3.79
	D_e	45.1	40.8	222.2	207.2
Refs. [3–5] [a]	R_e	4.2	3.45	4.5	3.9
	D_e	40.5	36.6	220.1	183.6

[a] More refined values are collected and critically analyzed in Ref. [4]. These refinements do not change the general picture discussed through the present comparison.

4. Results

4.1. The ground state

We compare the shapes of the $HeCl_2$ and $ArCl_2$ interaction potentials for the fixed Cl–Cl internuclear distance of 1.988 Å and regions of distances from Rg to the center of mass of Cl_2 up to 5 Å, for three treatments:

(A) isotropic pairwise additive atom–atom potentials, in which for the Rg–Cl interaction we use the ground state $^2\Sigma$ potential:

$$V = V^{ClCl} + \sum_{i=1,2} V^{RgCl}(R_i) . \tag{7}$$

(B) DIM surface limited to only neutral configurations, only the first four Cl_2 states in Table 1, in which the anisotropic Rg–Cl potentials are included. This is obtained as the lowest root of the 4×4 secular equation. Note, if only the diagonal matrix element H(4,4) of Table 1 is taken into account without any coupling to other states, then we would arrive at the Naumkin–Knowles (NK) model, where [17]:

$$V_{cov} = \sum_{i=1,2} \left[V_{\Pi}^{RgCl}(R_i) \sin^2 \phi_i + V_{\Sigma}^{RgCl}(R_i) \cos^2 \phi_i \right] . \tag{8}$$

(C) DIM surfaces with the inclusion of ion-pair states, obtained as the lowest root of the secular equation of the 10×10 matrix described in Eq. (1). The resulting potential energy surface can be formulated, to explicitly show the various contributions, through a procedure equivalent to what leads to the approximation of Eq. (8). This is accomplished by converting the 10×10 Hamiltonian matrix form the initial polyatomic basis set shown in Table 1, with mixings, to the set that diagonalizes the Cl_2 fragment Hamiltonian (with corresponding transformation of the $Rg–Cl_i$ matrices). Then, the neglect of couplings among the lowest energy matrix elements to all other states, leads to the following expression:

$$V = V_{cov} \cos^2 \beta + V_{ion} \sin^2 \beta , \tag{9}$$

where V_{cov} is given by Eq. (8), while:

$$V_{ion} = \Delta V_{ion} + \tfrac{1}{2} \left[\sum_{i=1,2} \left[V^{RgCl^+}(R_i) + V_{\Sigma}^{RgCl^-}(R_i) \right] \right] , \tag{10}$$

with ΔV_{ion} defined in Eq. (5), a single potential describes the closed shell-closed shell $Rg–Cl^-$ interaction (given in Table 3); while the closed shell–open shell interaction with the positive ion, $Rg–Cl^+$, is given as:

$$V^{RgCl^+}(R_i) = \frac{\left(3\cos^2 \phi_i - 1\right)^2}{4} V_{\Sigma}^{RgCl^+}(R_i) + 3\left(\sin^2 \phi_i \cos^2 \phi_i\right) V_{\Pi}^{RgCl^+}(R_i) + \frac{3\sin^4 \phi_i}{4} V_{\Delta}^{RgCl^+}(R_i) , \tag{11}$$

with parameters given in Table 3.

Fig. 2 shows contour plots of the ground state potential energy surfaces of $HeCl_2$ for the three treatments. The Cl_2 axis is placed along the horizontal, and the energy contours are drawn in 2 cm^{-1} increments starting from the surface minimum. Table 4 contains parameters of the stationary points of these surfaces. The comparison allows an assessment of the different contributions to the surface topology. The inclusion of the anisotropy of the Rg–Cl interaction (a vs. b) leads to the appearance of the linear well, however, this well is separated from the T-valley by an insignificant saddle point of less than 2 cm^{-1} in height. Inclusion of the ion-pair contributions (b vs. c) brings the wells closer in energy, by reducing the T-well minimum, while creating a well defined saddle point between the two minima. The main conclusion from this study is that the T-shaped and linear configurations of $HeCl_2$ become more competitive as one climbs from models A through C.

The calculation results for $ArCl_2$ are presented in Fig. 3 and in Table 4, in the same format used for $HeCl_2$. In this case the assessment of the effect of the ionic configuration is more obvious. Now, the DIM scheme with inclusion of ion-pair states predicts that the linear form of $ArCl_2$ is lower in energy. As before, the linear minimum already arises from the anisotropy of the Ar–Cl interaction (case B), although significantly less deep

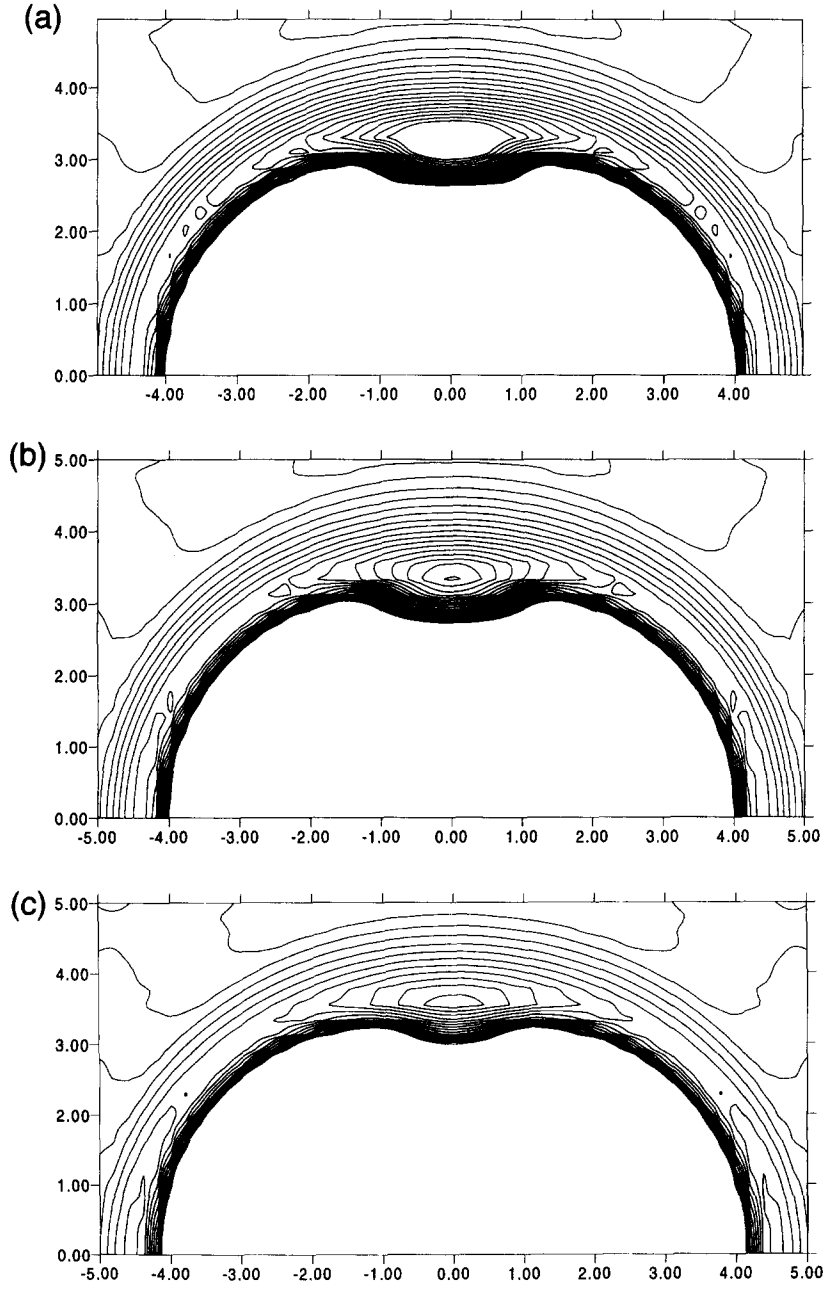

Fig. 2. Contour plots $HeCl_2$, plotted at 2 cm^{-1} resolution. Top panel: isotropic atom–atom potentials, scheme A of text; middle panel: DIM surface with only neutral Cl_2 states, scheme B of text; bottom panel: DIM surface including ion-pair state contribution, scheme C of text.

than the T-geometry. The linear well is stabilized, while at the same time the T-well is destabilized, when the ion-pair contribution is included.

In short, within the DIM formalism, the inclusion of ion-pair states into the set of polyatomic basis functions plays a direct role in controlling the balance between linear and T-shaped configurations of $Rg–Cl_2$ van der Waals complexes.

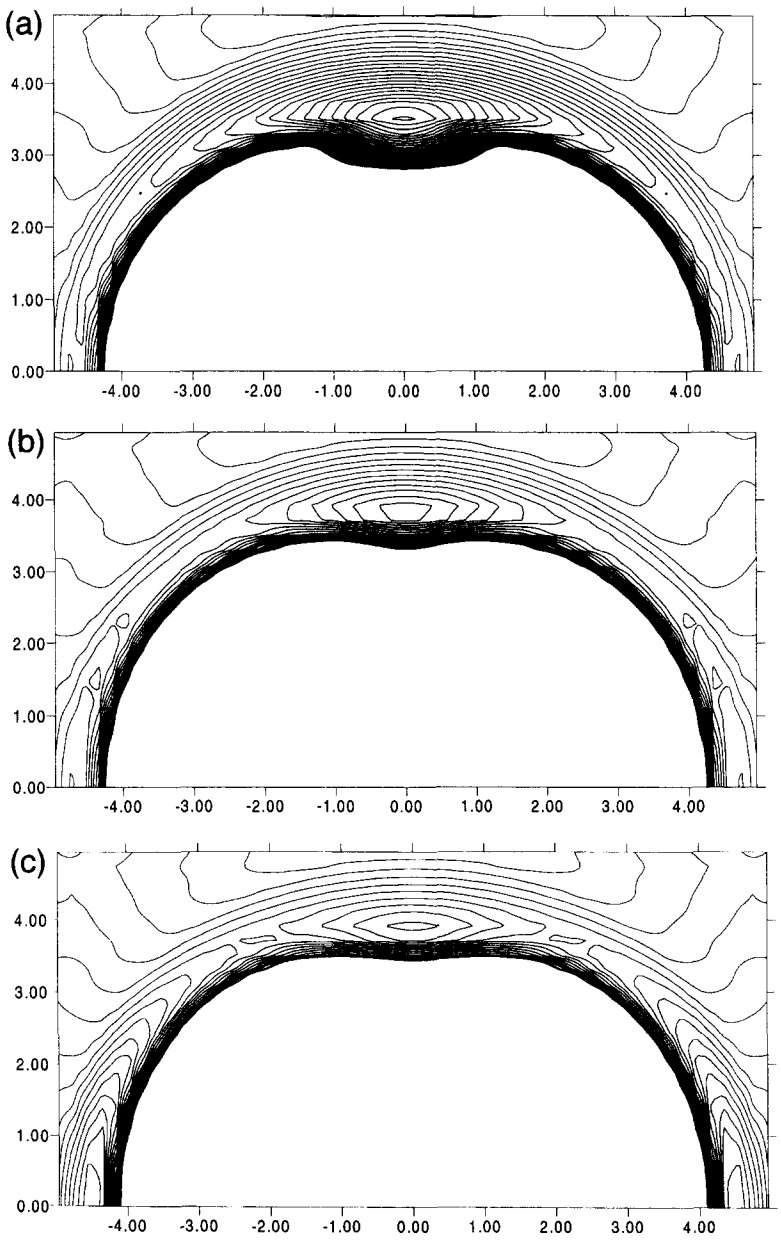

Fig. 3. Contour plots $ArCl_2(X\,^1\Sigma)$ plotted with 10 cm^{-1} resolution. Top panel: isotropic atom–atom potentials, scheme A of text; middle panel: DIM surface with only neutral Cl_2 states, scheme B of text; bottom panel: DIM surface including ion-pair state contribution, scheme C of text.

4.2. The excited state

Within the same approximation as above, it is possible to give an analytical expression for the excited state, $Cl_2(^3\Pi)$–Rg, potential energy surface. Starting with the 6×6 matrix in Table 1 (b), therefore limited to the single $Cl^+Cl^-(^3\Pi)$ ionic contribution. As before, the overall surface is given by the admixture of covalent and ionic contributions, of Eq. (9), except now the covalent contribution is isotropic, the average of Σ and Π interactions of Rg–X:

$$V_{\mathrm{cov}} = \tfrac{1}{2} \sum_{i=1,2} \left[V_{\Pi}^{\mathrm{RgCl}}(R_i) + V_{\Sigma}^{\mathrm{RgCl}} \right], \tag{12}$$

while the ionic contribution is given as:

$$V_{\mathrm{ion}} = \Delta V_{\mathrm{ion}} + \tfrac{1}{2}\Big[\sum_{i=1,2} \left[V_{\Pi}^{\mathrm{RgCl}^+}(R_i) + V_{\Sigma}^{\mathrm{RgCl}^-}(R_i) \right]. \tag{13}$$

where the $RgCl^+$ terms limited to the $^3\Pi$ curve. The resulting surface is shown in Fig. 4 for the case of $Cl_2(^3\Pi)$–Ar. Note, in this case, the inclusion of ionic configurations does not produce linear minima. The T-minimum in this case is at an internuclear distance of 3.6 Å, with a dissociation energy of 216 cm^{-1}.

4.3. The DIM insight

An attractive aspect of the DIM construct is that it provides simple insights about the final surfaces. To this end, we consider the hierarchy of effects.

First, let us consider neutral interactions alone. An $Rg–X_2$ surface based on isotropic Rg–X potentials would only have a T-shaped minimum, in which the Rg atom would have the benefit of stabilization by two X atoms via R^{-6} dispersion. The anisotropy of the Rg–X interaction results from the repulsive Pauli exclusion force. In the Σ state, where the halogen hole points at the Rg atom, a closer approach, and therefore deeper binding via dispersion is possible [20]. Since the Rg–X interaction is much weaker than the covalent bond in the molecular halogen, the quantization axis obtained by diagonalization of the DIM matrix remains essentially unaffected by Rg. Accordingly, in the $^1\Sigma$ ground state, the p_z hole on each of the halogens implies dimples in the electron density for linear approach of the rare gas. This is the essence of V_{cov} in Eq. (8). Whether linear minima will result, depends on whether the anisotropy of the Rg–X potentials, i.e., the difference between Σ and Π approaches, is large enough to overcome the double coordination in the T-geometry. This does not occur in $He–Cl_2$ and $Ar–Cl_2$. In the excited $^3\Pi$ state of X_2, the hole on each X atom has an equal contribution from p_x and p_z, hence the Rg–X interaction is isotropic, the average of Π and Σ potentials, as in Eq. (12). Accordingly, the minimum in the three-body excited surface would be exclusively limited to the T-geometry.

The inclusion of ionic configurations incorporates weighted contributions from the atom–ion pair potentials. We need only focus on the anisotropic $Rg–X^+$ fragment, in which the interactions are a balance of electrostatic

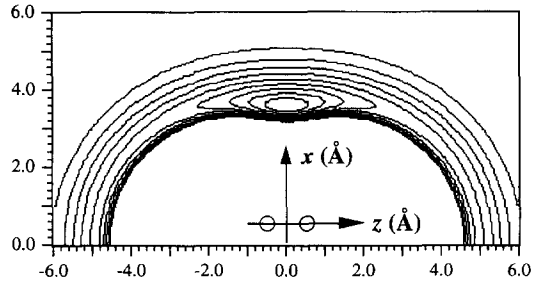

Fig. 4. Contour plots $ArCl_2(X\,^3\Pi)$ plotted with 20 cm^{-1} resolution.

attraction and Pauli repulsion. Since Rg represents a spherical charge distribution, the anisotropy is strictly the result of the repulsion. Thus, the dramatic difference among $^1\Sigma$, $^1\Pi$, $^1\Delta$ potentials of Ar–$Cl^+(^1D)$, see Table 2, is the result of Ar approaching a doubly unoccupied, singly occupied, or doubly occupied orbital, respectively. The same consideration explains the similarity between $^1\Pi$ and $^3\Pi$ states, and $^1\Delta$ and $^3\Sigma$ states [22]. It is the contribution of the Rg–$Cl^+(^1\Sigma)$ potential, which is bound by nearly 1.5 eV, that leads to the generation of the linear minimum in the singlet ground state. Also, the absence of binding in $RgCl^+(^3\Sigma)$ while $RgCl^+(^3\Pi)$ is bound by ≈ 0.3 eV, simply reinforces the T-shaped minimum on the triplet surface when the ionic admixture is added.

5. Discussion and conclusions

The general features of the ground state potential energy surfaces of He–Cl_2 and Ar–Cl_2 obtained by the inclusion of ionic configurations in the DIM basis seem realistic in that they show similar stabilities for the linear and T-geometries of the complex, a feature that is absent when only neutral interactions are considered in the most thorough treatment [17]. The ion-pair states give the effect sought on the topology of the surface, and account for the recognized non-additivity of pair interactions. In comparison to the best ab initio surfaces, the deviations in the constructed surfaces range from ≈ 10–50 cm^{-1} for the various stationary points that are compared in Table 4. There is no comparable ab initio data for the excited state. Spectroscopically, it is known that the T-minimum in the $B(^3\Pi_u)$ state is ≈ 12 cm^{-1} shallower than in the ground state [29]. Using the converged values between experiment and highest level of theory for the ground state [4], we can back track a binding energy of ≈ 200 cm^{-1} for the excited state minimum, to be compared with 216 cm^{-1} in the present (a 5% deviation). Since the DIM predictions are critically dependent on the quality of the diatomic input, an assessment of their accuracy is useful for putting the observed deviations in perspective.

The most accurate of the input potentials used are the Rg–Cl adiabatic curves for Σ and Π states, which are derived by Aquilanti et al. from experiments, and which are significantly more accurate than the observed deviations [20]. The closed shell Rg–Cl^- potentials are also deemed reliable. Nevertheless, the He–Cl^- potential used here has been criticized by Diercksen and Sadlej [27]. They noted that the long-range part of this potential was based on outdated and under estimated polarizabilities for Cl^-. However, due to cancellation of errors, the final parameters for the He–Cl^- interaction were considered satisfactory. Relying on the careful analysis of He–F^- and He–Cl^- by Dierksen and Sadlej [26,27], we estimate possible errors of order 10–50 cm^{-1} in the range of interest to our calculations. The Rg–Cl^+ potentials are subject to the largest errors. The singlet states correlating with the Ar + $Cl^+(^1D)$ dissociation limit were previously computed using first order CI [22]. We repeated these calculations by dramatically extending the configuration space. The differences in interaction energies in the two procedures was $\approx 20\%$, which corresponds to uncertainties of several hundred wavenumbers in the range of interest in the present. Thus, the deviations of the devised surfaces from the best ab initio results are well within the uncertainties of the input parameters in our construct.

Despite the uncertainties in diatomic input energies, the qualitative conclusions of the DIM predictions remain firm. Even assuming severe modifications in fragment potentials the energies of linear and T-shaped forms of $HeCl_2$ become competitive upon inclusion of ion-pair contributions. What is affected by the possible modifications of the energies of diatomic fragments are the precise values of binding energies of $HeCl_2$, within 10 cm^{-1}. For ground state $ArCl_2$ the conclusion of the greater stability of the linear form in the DIM treatment we deem to be outside the possible errors in the diatomic input. Similarly, the absence of the linear minima in the excited state is a reliable conclusion. These features are absent in DIM surfaces, such as the recent work of Buchachenko and Stepanov [30], in which ionic configurations are ignored. Quite clearly the details of the surface topology can be modified by a suitable adjustment of input parameters, or alternatively, the functional form of Eq. (9) can be used as a fitting scheme to generate surfaces for applications requiring high accuracy.

What concerns condensed phase applications, where many-body contributions control structure and dynamics, it is important to have surfaces that have properly parametrized non-additivity. The present approach seems

quite promising in that respect. In such applications, the mixing coefficient β should be interpreted as a second order coupling between neutral and ionic states. Accordingly, given the differential solvation of ionic and neutral surfaces in dielectric media, the ionic admixture in neutral configurations will increase, with inverse proportionality to the difference between ionic and neutral surfaces. Indeed, in recent studies of $Xe-Cl_2$ complexes in liquid Ar, a strongly bound linear complex is inferred both in the ground, X, and excited, A, states of the molecule [31]. Finally, we point out that in addition to structure, the scheme proposed here makes predictions with respect to nonadiabatic dynamics, through the effect of ionic configurations on nondiagonal matrix elements of the DIM Hamiltonian. Thus, we expect rigorous tests of the formulation advanced here to arise in studies of solvent induced predissociation dynamics, such as that of I_2 isolated in rare gas matrices an initial study of which has already been reported [32].

Acknowledgements

This research was supported in part by the Russian Basic Research Foundation (Grant No. 96-03-32284), and in part by the US Air Force Office of Scientific Research (Grant No. F49620-95-1-0213).

References

[1] K. Morokuma, J. Chem. Phys. 55 (1971) 1236.
[2] A.E. Reed, L.A. Curtiss, F. Weinhold, Chem. Rev. 88 (1988) 899.
[3] S.S. Huang, C.R. Bieler, K.C. Janda, F.-M. Tao, W. Klemperer, P. Casavecchia, G.G. Volpi, N. Halberstadt, J. Chem. Phys. 102 (1995) 8846.
[4] J. Williams, A. Rohrbacher, D. Djahandideh, K.C. Janda, A. Jamka, F. Tao, N. Halberstadt (submitted).
[5] F.-M. Tao, W. Klemperer, J. Chem. Phys. 97 (1992) 440.
[6] G. Chalasinski, M. Gutowski, M.M. Szczesniak, J. Sadlej, S. Scheiner, J. Chem. Phys. 101 (1994) 6800.
[7] S.M. Cybulski, R. Burcl, G. Chalasinski, M.M. Szczesniak, J. Chem. Phys. 101 (1994) 6800.
[8] J. Sadlej, G. Chalasinski, M.M. Szczesniak, J. Mol. Struct. (THEOCHEM) 307 (1994) 187.
[9] B.L. Grigorenko, A.V. Nemukhin, A.A. Buchachenko, N.F. Stepanov, S. Ya. Umanskii, J. Chem. Phys. (in press).
[10] A.V. Nemukhin, N.F. Stepanov, Int. J. Quant. Chem. 15 (1979) 49.
[11] S.V. Ljudkovski, A.V. Nemukhin, N.F. Stepanov, J. Mol. Struct. 67 (1980) 81.
[12] I. Last, T.F. George, J. Chem. Phys. 87 (1987) 1183.
[13] I. Last, T.F. George, M.E. Fajardo, V.A. Apkarian, J. Chem. Phys. 87 (1987) 5917.
[14] I. Last, T.F. George, J. Chem. Phys. 98 (1993) 6406.
[15] B.L. Grigorenko, A.V. Nemukhin, V.A. Apkarian, J. Chem. Phys. 104 (1996) 5510.
[16] A.V. Nemukhin, B.L. Grigorenko, A.V. Savin, Chem. Phys. Lett. 250 (1996) 226.
[17] F.Yu. Naumkin, P.J. Knowles, J. Chem. Phys. 103 (1995) 3392.
[18] J. Tully, in: Modern Theoretical Chemistry, Semiempirical Methods of Electronic Structure Calculations, Vol. 7A, G.A. Segal (Ed.), Plenum Press, New York, 1977, ch. 6.
[19] I.H. Gersonde, H. Gabriel, J. Chem. Phys. 98 (1993) 2094.
[20] V. Aquilanti, D. Cappelelletti, V. Lorent, E. Luzzatti, F. Pirani, J. Phys. Chem. 97 (1993) 2063.
[21] R. Ahlrichs, H.J. Bohm, S. Brode, K.T. Tang, J.P. Toennies, J. Chem. Phys. 88 (1988) 6290.
[22] K. Balasubramanian, P. Feng, J.J. Kaufman, P.C. Hariharan, W.S. Koski, Phys. Rev. A 37 (1988) 3204.
[23] L.F. Pacios, P.A. Christiansen, J. Chem. Phys. 82 (1985) 2664.
[24] M.W. Schmidt, K.K. Baldridge, J.A. Boatz, J.H. Jensen, S. Koseki, M.S. Gordon, K.A. Nguyen, T.L. Windus, S.T. Elbert, Quantum Chemistry Program Exchange Bulletin, 1990, 52.
[25] D. Staerk, S.D. Peyrimhoff, J. Mol. Struct. (THEOCHEM) 150 (1987) 203.
[26] G.H.F. Diercksen, A.J. Sadlej, Chem. Phys. Lett. 156 (1989) 269.
[27] G.H.F. Diercksen, A.J. Sadlej, Chem. Phys. 131 (1989) 215.
[28] S.D. Peyerimhoff, R.J. Buenker, Chem. Phys. 57 (1981) 279.
[29] D.D. Evard, C.R. Bieler, J.I. Cline, N. Sivakumar, K.C. Janda, J. Chem. Phys. 89 (1988) 2829.
[30] A.A. Buchachenko, N.F. Stepanov, Chem. Phys. Lett. 261 (1996) 591.
[31] M.W. Hill, V.A. Apkarian, J. Chem. Phys. 105 (1996) 4023.
[32] R. Zadoyan, M. Sterling, V.A. Apkarian, J. Chem. Soc. Faraday Trans. 92 (1996) 1821.